Teeri, T., Lehtovaara, P., Kaupinen, S., Salovouri, I., & Knowles, J. (1987) *Gene 51*, 43–52.
Tomme, P., Van Tilbeurgh, H., Pettersson, G., Vandekerckhove, J., Knowles, J., & Teeri, T. (1988) *Eur. J. Biochem. 170*, 575–581.
Tüchsen, E., & Woodward, C. (1987) *Biochemistry 26*, 1918–1925.
Van Tilbeurgh, H., Tomme, P., Caleyssens, M., Bhikhabhai, R., & Pettersson, G. (1986) *FEBS Lett. 204*, 223–227.
Venkatachalam, C. M. (1968) *Biopolymers 6*, 425–436.
Wagner, G., Neuhaus, D., Wörgötter, E., Vasák, M., Kägi, J. H. R., & Wüthrich, K. (1986) *J. Mol. Biol. 187*, 131–135.
Wagner, G., Braun, W., Havel, T. F., Schaumann, T., Go, N., & Wüthrich, K. (1987) *J. Mol. Biol. 196*, 611–639.
Westergren, C., Pettersson, G., Knowles, J., & Jones, T. A. (1989) *J. Mol. Biol.* (in press).
Williamson, M. P., Havel, T. F., & Wüthrich, K. (1985) *J. Mol. Biol. 182*, 295–315.
Wlodawer, A., Walter, J., Huber, R., & Sjölin, L. (1984) *J. Mol. Biol. 180*, 301–329.
Wüthrich, K. (1986) *NMR of Proteins and Nucleic Acids*, Wiley, New York.
Wüthrich, K., Billeter, M., & Braun, W. (1983) *J. Mol. Biol. 169*, 949–961.
Wüthrich, K., Billeter, M., & Braun, W. (1984) *J. Mol. Biol. 180*, 715–740.
Zuiderweg, E. R. P., Boelens, R., & Kaptein, R. (1985) *Biopolymers 24*, 601–611.

# Zinc Environment in Sheep Liver Sorbitol Dehydrogenase†

Martinus C. Feiters*,‡ and Jonathan Jeffery§

*Department of Bioorganic Chemistry, State University of Utrecht, Padualaan 8, P.O. Box 80.075, NL-3508 TB Utrecht, The Netherlands, and Department of Biochemistry, University of Aberdeen, Marischal College, Aberdeen AB9 1AS, Scotland, United Kingdom*

*Received February 6, 1989; Revised Manuscript Received May 19, 1989*

ABSTRACT: The extended X-ray absorption fine structure (EXAFS) associated with the zinc K-absorption edge has been recorded for sorbitol dehydrogenase. It is interpreted in terms of one cysteine sulfur among the ligands to the active site zinc atom. Simulations of the EXAFS based on the presence of two such sulfurs are less satisfactory, and comparison with the EXAFS of such systems points to the presence of only one sulfur ligand in sorbitol dehydrogenase. These results provide evidence that sorbitol dehydrogenase does not have the characteristic one water, one His, two Cys arrangement of ligands to the active site zinc found in the homologous alcohol dehydrogenases and are consistent with the one water, one His, one Cys, one Glu ligand arrangement of the proposed model of sorbitol dehydrogenase [Eklund, H., Horjales, E., Jörnvall, H., Brändén, C.-I., & Jeffery J. (1985) *Biochemistry 24*, 8005–8012]. Evidence for the correctness of the model is also evidence for validity of predictive techniques used in constructing the model, i.e., computer graphics fitting of the amino acid sequence to the crystallographically derived structure of a different but homologous protein.

The amino acid sequence of sheep liver sorbitol dehydrogenase (Jeffery et al., 1984a) has been aligned with those of mammalian, plant, fungal, and yeast alcohol dehydrogenases, clearly establishing that they are homologous proteins (Jörnvall et al., 1984, 1987; Eklund et al., 1985). Sorbitol dehydrogenase is a zinc enzyme (Jeffery et al., 1984b), as are the homologous alcohol dehydrogenases. The protein ligands to the active site zinc atom of these alcohol dehydrogenases are one His and two Cys (His-67, Cys-46, and Cys-174 in the numbering system of the horse liver enzyme; Brändén et al., 1975). The fourth ligand is water, or substrate during the reaction process.

A model has been constructed for the three-dimensional structure of sorbitol dehydrogenase by fitting the amino acid sequence to the crystallographically determined tertiary structure of horse liver alcohol dehydrogenase (Eklund et al., 1985). According to this model, the protein ligands to the active site zinc atom in sorbitol dehydrogenases are one His, one Cys, and one Glu (His-68, Cys-43, and Glu-154 in the continuous numbering system of sorbitol dehydrogenase; Jeffery et al., 1984a; Karlsson et al., unpublished data). In this part of the polypeptide chain, neither the Cys nearest to Glu-154 (Cys-163), which is the Cys that could be considered to be a candidate for coordination to zinc with another alignment (Eklund et al., 1985), nor the next-nearest Cys (Cys-138), which is not conserved in the alcohol dehydrogenases, is positioned in the model in a way that would allow it to serve as a zinc ligand. The fourth ligand in the model is a water molecule (or substrate during the reaction process), and a further water molecule is thought possibly to

† This work was supported by the British Science and Engineering Research Council (SERC), providing funds to the University of Manchester to establish the EXAFS service, with experimental and computational facilities at the SERC Daresbury Laboratory. General financial support by the University of Manchester and the University of Aberdeen is gratefully acknowledged. This work was carried out under SERC Grant GR/D 44188.

* Correspondence should be addressed to this author.
‡ University of Utrecht.
§ University of Aberdeen.

0006-2960/89/0428-7257$01.50/0 

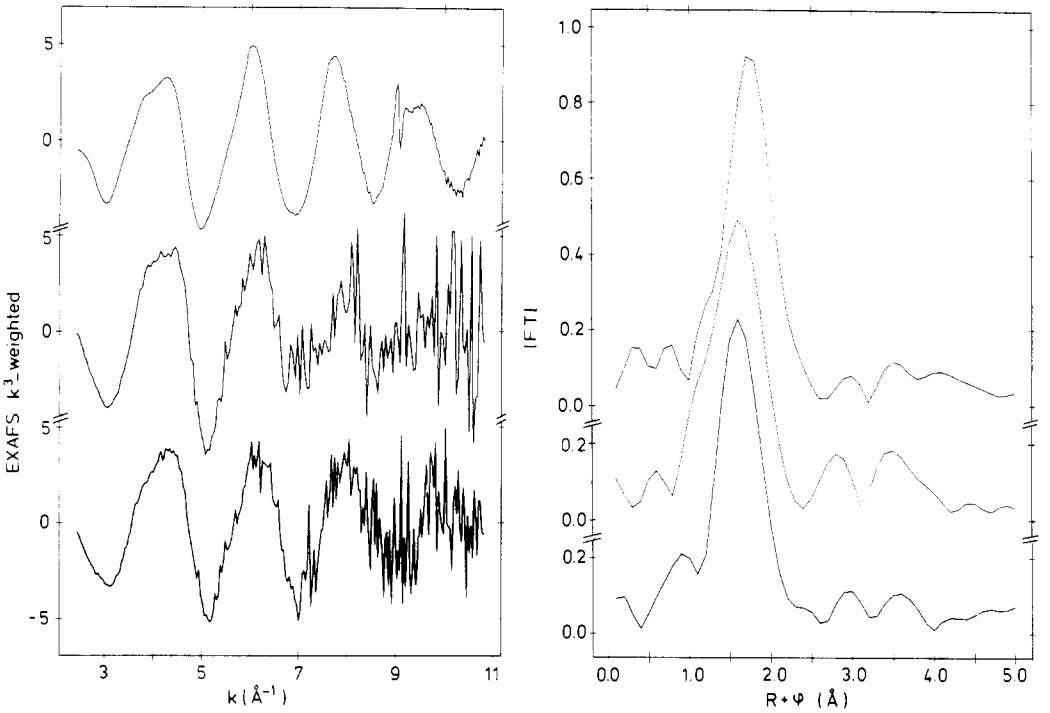


FIGURE 1: $k^3$-weighted EXAFS (left panel) and Fourier transforms (right panel, not phase corrected) of (1,10-phenanthroline)bis(4-toluenethiolato)zinc(II) (I) (upper traces) and sorbitol dehydrogenase at 277 K (middle traces) and 77 K (bottom traces).

be present in the absence of substrate and to interact with Lys-293 and Glu-154. The model accounts for distinctive functional characteristics of sorbitol dehydrogenase (Eklund et al., 1985) and helps understanding of structure–function relationships among polyol and alcohol dehydrogenases generally (Jeffery & Jörnvall, 1988). However, direct experimental evidence for the correctness of the model has been lacking.

Studies of the extended X-ray absorption fine structure (EXAFS) at the zinc K-absorption edge of metalloproteins have in recent years contributed to the identification of metal ligands in zinc proteins (Garner & Feiters, 1987). The oscillations in the X-ray absorption coefficient after the zinc K-edge step are described by interference effects on the central absorber zinc atom, due to the fact that the photoelectron wave leaving the excited zinc atom is backscattered by the zinc ligands (Stern, 1974). Phase-corrected Fourier transformation of the EXAFS with respect to $\exp(-i2kR)$, where $R$ is the absorber–backscatterer distance, gives the radial distribution function around the absorber (Sayers et al., 1971). From analysis of the EXAFS, ligand distances and first-shell coordination numbers may be derived with accuracies of ±0.02 Å (Citrin et al., 1976) and 20% (Eisenberger & Lengeler, 1980), respectively. Because the backscattering amplitude of sulfur is approximately $\pi$ out of phase with those of carbon, nitrogen, and oxygen, if placed at the same distance, it is easy to distinguish sulfur from any of those (Hasnain et al., 1985) but difficult to discriminate between the latter three, commonly referred to as low-$Z$ ligands. In this way, it has been possible to classify zinc sites in proteins (Garner & Feiters, 1987) on the basis of their ligands as derived from EXAFS: type A [sulfur ligands only, e.g., metallothionein (Abrahams et al., 1986) and "structural" sites of liver alcohol dehydrogenase (Zeppezauer et al., 1986) and aspartate transcarbamylase (Phillips et al., 1982)], type B [sulfur and nitrogen/oxygen ligands, e.g., transcription factor (Diakun et al., 1986)], and type C [nitrogen/oxygen ligands only, e.g., phospholipase C (Feiters et al., 1986a)]. On the basis of the model discussed above, the zinc site in sorbitol dehydrogenase is expected to be of type B. The aim of the present EXAFS study of sorbitol dehydrogenase was not only to investigate this but also to determine whether the ligands to zinc atom include two sulfur ligands (as in the homologous alcohol dehydrogenases) or only one (as in the sorbitol dehydrogenase model). The results are shown to favor the latter.

## Materials and Methods

*Protein Preparation.* Sheep liver sorbitol dehydrogenase, prepared as described earlier (Jeffery et al., 1981), was concentrated by ultrafiltration at 1 °C to obtain concentrations in the range 50–150 mg/mL. For EXAFS measurements, cells of 2.5-mm light path were used.

*EXAFS Data Collection.* X-ray fluorescence spectra at the Zn K-edge were measured in two sessions, one using EXAFS station 7.1 and the other using wiggler line EXAFS station 9.2 of the SERC Synchrotron Radiation Source, operating at 2.0 GeV with an average current of 200 mA. The experiment on 7.1 was carried out at ~277 K, with the experimental setup for fluorescence detection with thallium-doped sodium iodide scintillation counters described earlier (Hasnain et al., 1984). A premonochromator toroidal mirror was used to focus the beam at the sample position, not reflecting radiation with wavelength < 1.2 Å and rejecting harmonics. The experiment on 9.2 was carried out at ~77 K, with an Oxford Instruments liquid helium fluorescence EXAFS cryostat and a setup with individual electronics for every detector as described elsewhere (Baines et al., 1986). The double-crystal order-sorting monochromator (Greaves et al., 1983) was set to 50% harmonic rejection. In both sessions, replicate spectra were recorded and averaged. Enzymic activity was retained during EXAFS data collection. EXAFS transmission data of (1,10-phenanthroline)bis(4-toluenethiolato)zinc(II) (I) (kindly provided by Prof. C. D. Garner, Department of Chemistry, University of Manchester) and zinc sulfide (II) were collected in transmission mode at ambient temperature.

*EXAFS Data Analysis.* The programs used for EXAFS data analysis are available from the Synchrotron Radiation Source Programme Library, Daresbury Laboratory, War-

rington WA4 4AD, U.K. After background subtraction, with the program EXBACKI written by I. Ross, the EXAFS was transformed into $k$ space with

$$k = [2m(E - E_0)/\hbar^2]^{1/2}$$

where $E$ and $E_0$ are the energies of the incident beam and of the relevant absorption edge, respectively. Fourier transforms were calculated with respect to $\exp(-i2kR)$, where $R$ is the distance of a scattering atom from the central atom. Phase shifts and backscattering factors were calculated by the MUFFPOT program, using Clementi-Roetti wave functions for scattering atoms in the neutral state and approximating the excited zinc atom by the wave function of neutral gallium with one electron removed from the 1s orbital. Best results for the main shell of zinc sulfide were obtained when a double-positive charge was placed on the central atom in the MUFFPOT calculations, in agreement with results for zinc imidazole model compounds (Feiters et al., 1986a; M. C. Feiters and C. Little, unpublished data).

EXAFS spectra were fitted with the fast curved-wave program EXCURVE (Gurman et al., 1984, 1986). The quality of the simulations was assessed by visual comparison of the experimental and simulated EXAFS and their Fourier transforms and by calculation of the difference function, further referred to as fit index. The imaginary potential, describing the electron wave lifetime, and the amplitude reduction factor, correcting for multiple excitation effects, were set to −1.0 eV and 0.7, respectively, and not further refined. $\Delta E_0$, representing the photoelectron energy as $k = 0$, was set to the value it refined to in the analysis of the EXAFS of tetrakis(imidazole)zinc(II) diperchlorate (III) EXAFS, viz., 27.52 eV (Feiters et al., 1986a; M. C. Feiters & C. Little, unpublished data). However, since it refined to a lower value in the analysis of zinc sulfide (II) EXAFS, $\Delta E_0$ was appropriately shifted for sulfur contributions. Analysis of Fourier-filtered main shells was carried out in $k^3$ weighting, refining the distances $R$ and the Debye–Waller-type factors $a$ ($=2\sigma^2$, in Å$^2$), iteratively. Detailed analysis of the full, non-Fourier-filtered spectrum was carried out in $k^2$ weighing, also by refining the distances $R$ and the Debye–Waller-type factors. Occupancies were only allowed to take integer values and were varied in steps.

## Results and Discussion

The EXAFS and corresponding Fourier transforms are shown in the lower two traces in the left and right panels of Figure 1 for sorbitol dehydrogenase at 277 K (18 scans) and at 77 K (7 scans). The EXAFS spectra show very similar beating patterns but some difference in the shape of the EXAFS at 5 Å$^{-1}$, as well as differences in amplitude close to 4 and 6 Å$^{-1}$ (277 K greater) and also near to 7.5 and 8.5 Å$^{-1}$ (77 K greater). The Fourier-transform peak is at the same position but narrower at the lower temperature.

These data for sorbitol dehydrogenase are compared to the EXAFS of I (Figure 1, upper traces), for which a crystal structure is available (Cremers et al., 1980), and of the transcription factor IIIA protein (Figure 2), for which data were kindly made available to us by Dr. G. P. Diakun (Daresbury Laboratory) and Dr. L. Fairall and Dr. A. Klug (MRC Molecular Biology Laboratory, Cambridge, U.K.) before publication (Diakun et al., 1986). In the reference compound I, the zinc atom has two nitrogen ligands at 2.112 Å and two sulfur ligands at 2.261 Å (Cremers et al., 1980); in the transcription factor, the proposed ligands to the zinc atom are two nitrogen (His) and two sulfur (Cys), which is

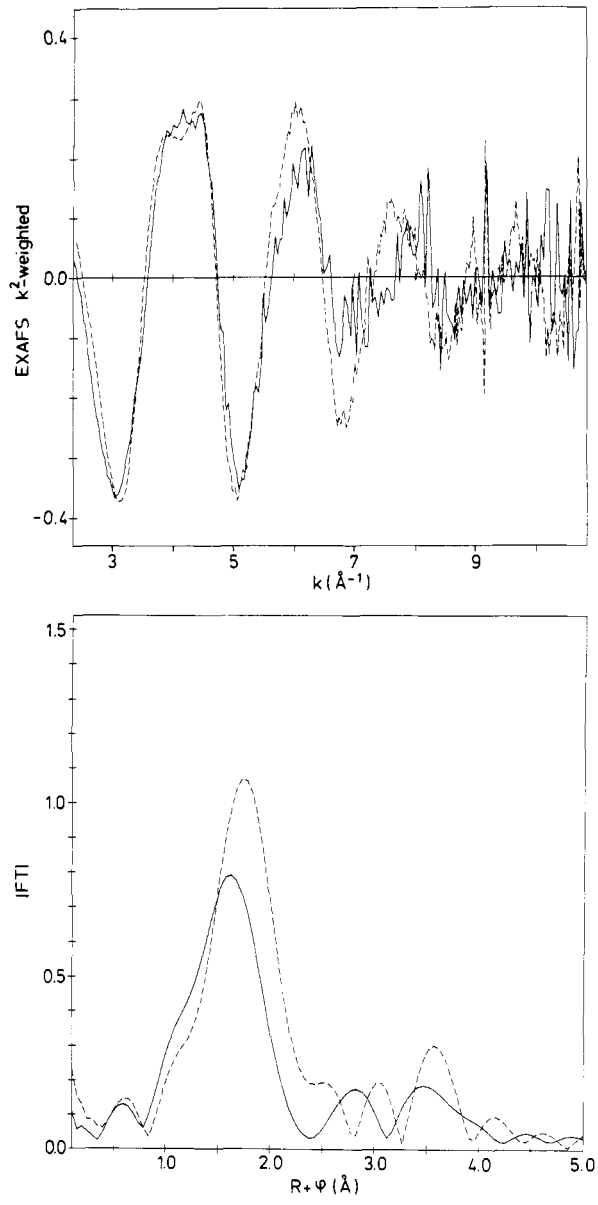


FIGURE 2: $k^2$-weighted EXAFS (upper panel) and Fourier transform (bottom panel, not phase corrected) of sorbitol dehydrogenase at 277 K (solid line) and transcription factor TF IIIA at ambient temperature [dashed line; data kindly made available by Drs. G. P. Diakun, L. Fairall, and A. Klug (Diakun et al., 1986)].

consistent with the EXAFS (Diakun et al., 1986). Thus, from comparison of the sorbitol dehydrogenase EXAFS with the EXAFS of these zinc sites (Figures 1 and 2), the lower amplitude in the region above 6 Å$^{-1}$ and the difference in the Fourier transforms strongly indicate that sorbitol dehydrogenase has fewer than two sulfur ligands.

This suggestion is borne out by our EXAFS simulations. Our iteratively refined calculations of II and III (not shown) gave excellent agreement (±0.02 Å) with the crystallographic data for the main shells. The EXAFS of I could be satisfactorily modeled with the parameters at their crystallographic values. However, as in the protein, the main shell of this model is composed of unresolved low-$Z$ and sulfur ligand contributions, which are at similar distances and therefore have a tendency to interfere destructively, because of their opposite phases as mentioned earlier. As a result, we have noted high correlations between the refined parameters, a strong influence of $\Delta E_0$ on the relative size of the low-$Z$ and sulfur contributions, and a tendency for high occupancy values which are not physically resonable. Destructive interference of sulfur and

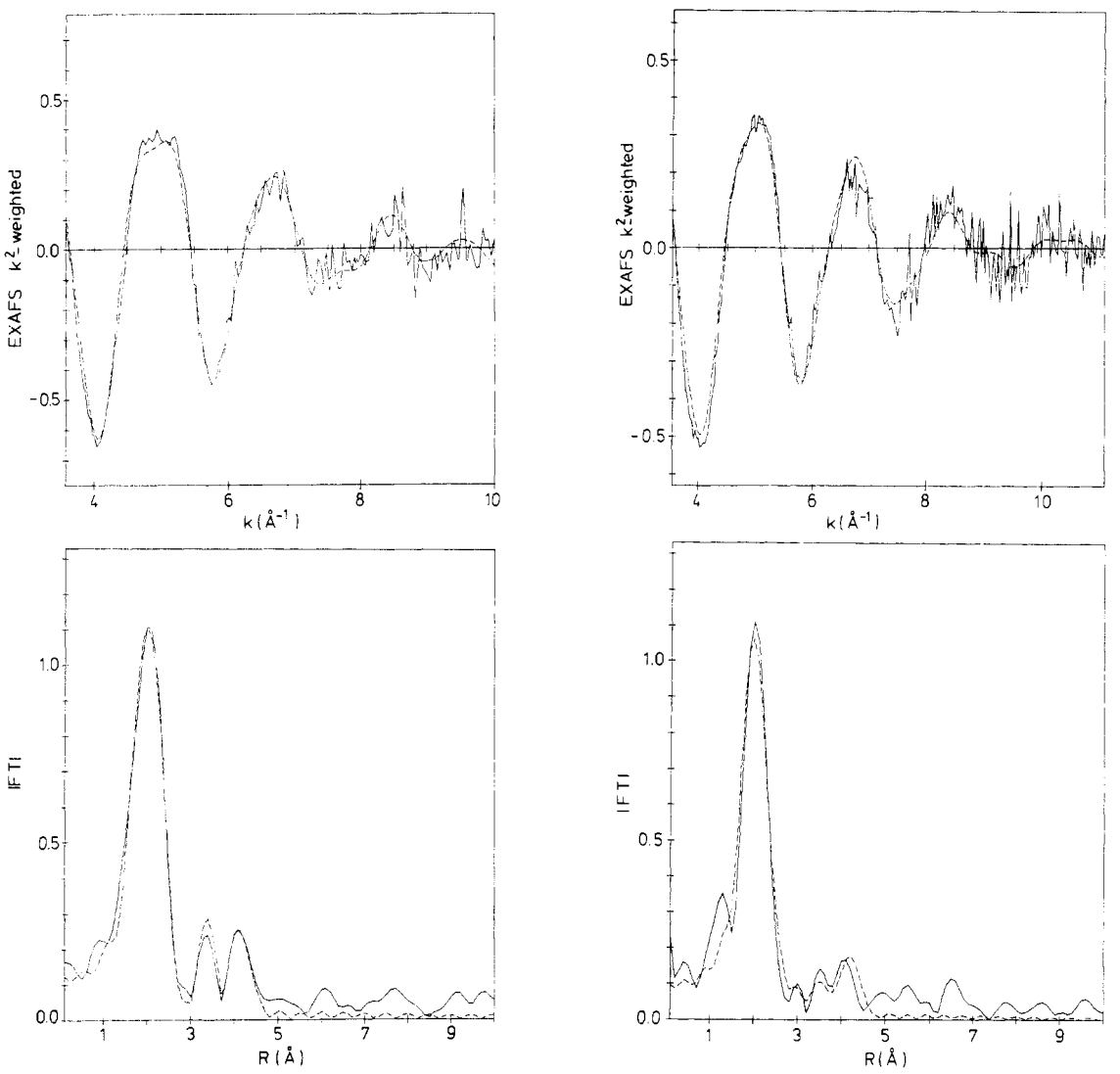


FIGURE 3: Experimental (solid lines) and simulations (dashed lines, parameters in Table II) of the $k^2$-weighted EXAFS (upper panels) and Fourier transforms (lower panels, phase corrected) of sorbitol dehydrogenase at 277 K (left panels) and 77 K (right panels).

low-$Z$ shells has been implicated in EXAFS studies of blue copper proteins (Groeneveld et al., 1986) and model compounds for them (Feiters et al., 1986b). High occupancy values which are not physically reasonable have been encountered in the analysis of the EXAFS of the complex of carbonic anhydrase and chloride anion (Yachandra et al., 1983), presumably because of interference of the low-$Z$ protein ligands with chlorine, whose backscattering amplitude and phase are similar to those of sulfur. Therefore, we have kept $\Delta E_0$, as well as the overall coordination number, at reasonable fixed values (see Materials and Methods) and varied the occupancies in steps, rather than allowing them to float. For the interpretation of the sorbitol dehydrogenase EXAFS, we have made simplifying assumptions concerning the structural possibilities to be distinguished, which are relatively clearcut.

Both the full spectra (in $k^2$ weighting) and Fourier-filtered main shells (in $k^3$ weighting) were simulated, refining distances and Debye–Waller-type factors, by starting from an arrangement of four-coordinated zinc having one sulfur ligand and three low-$Z$ ligands (i.e., oxygen or nitrogen ligands) or having two sulfur ligands and two low-$Z$ ligands. For both the 277 and the 77 K data and both the full spectra and the Fourier-filtered main shells, the fit indices (Table I) reached lower values (that is, better fits) with the refined simulations based on the one sulfur, three low-$Z$ ligand arrangement than with those based on the two sulfur, two low-$Z$ ligand arrangement. To this extent, the position is clear; the sorbitol dehydrogenase EXAFS is less well reconciled with the two sulfur (Cys), one nitrogen (His), one oxygen (water) ligand arrangement characteristic of the active site zinc of homologous alcohol dehydrogenases than with the one sulfur (Cys), one nitrogen (His), two oxygen (one water and one Glu) ligand arrangement proposed, on other grounds, for sorbitol dehydrogenase (Eklund et al., 1985).

However, the EXAFS data agree even better with simulations for five-coordinated zinc than for the four-coordinated zinc considered so far. Also in this case, as can be seen in Table I, the simulation with only one sulfur ligand (and four low-$Z$ ligands) is more favorable than that with the two sulfur ligands (and three low-$Z$ ligands). The best fits using five-coordination are presented in Figure 3 with the parameters used for the simulations in Table II. The minor shells at 3–4 Å are conceived as originating from backscattering by atoms in the imidazole ring. However, because of multiple scattering in this system, analysis of the occupancies and distances for these shells by single-scattering approximation is not expected to give reliable values (Pettifer et al., 1986; Strange et al., 1987; Feiters et al., 1988). Therefore, while contributions from such shells constitute evidence for the presence of imidazole ligands, they do not define the number of such ligands, which could be more than the one imidazole proposed in the model (Eklund et al., 1985).

Table I: Fit Indices of Best Simulations to Sorbitol Dehydrogenase EXAFS in $k^3$ Weighting (Fourier-Filtered Main Shells) or $k^2$ Weighting (Full, Non-Fourier-Filtered Spectra)[a]

| | Fourier-filtered main shell, $k^3$ weighting | | full spectra, $k^2$ weighting | |
|---|---|---|---|---|
| temp (K) | 277 | 77 | 277[b] | 77[c] |
| range of fit (eV) | 19–450 | 18–450 | 21–358 | 20–450 |
| Fourier-filter window (Å) | 0.5–2.4 | 0.4–2.3 | | |
| 4-coordination | | | | |
| 2 S + 2 low $Z$ | 2.69 | 2.16 | 0.53 | 0.42 |
| 1 S + 3 low $Z$ | 1.64 | 1.07 | 0.36 | 0.32 |
| 5-coordination | | | | |
| 2 S + 3 low $Z$ | 1.46 | 1.40 | 0.33 | 0.31 |
| 1 S + 4 low $Z$ | 0.78 | 0.80 | 0.26 | 0.26 |

[a] S, sulfur ligand; low $Z$, nitrogen or oxygen ligand. The windows for Fourier filtering are given as the nonphase-corrected distance $R'$. [b] Figure 3, left panels. [c] Figure 3, right panels.

Table II: Parameters Used for the Simulations of the EXAFS in the Left and Right Panels of Figure 3 (Sorbitol Dehydrogenase at 277 and 77 K, Respectively)[a]

| | left panels of Figure 3 | | | right panels of Figure 3 | | |
|---|---|---|---|---|---|---|
| atom type | Nr | $R$ | $2\sigma^2$ | Nr | $R$ | $2\sigma^2$ |
| O | 4 | 1.97 (2) | 0.010 (1) | 4 | 1.99 (2) | 0.013 (1) |
| S | 1 | 2.33 (2) | 0.002 (1) | 1 | 2.30 (3) | 0.014 (3) |
| C | 3 | 2.89 (3) | 0.009 (4) | 4 | 3.00 (3) | 0.020 (8) |
| C | 4 | 3.13 (2) | 0.017 (3) | 3 | 3.22 (4) | 0.02 (1) |
| N | 5 | 4.27 (3) | 0.012 (4) | 3 | 4.28 (3) | 0.007 (6) |
| FI | | 0.25845 | | | 0.26194 | |

[a] $\Delta E_0$, 27.52 eV; Nr, occupancy; $R$, distance to Zn (Å); Debye–Waller-type factor, given as $2\sigma^2$ (Å$^2$). O, oxygen; S, sulfur; C, carbon; N, nitrogen. FI, fit index ($k^2$ weighting).

Thus, a ligand arrangement of one sulfur and four low-$Z$ ligands presently provides the best fit for the observed EXAFS of sorbitol dehydrogenase, at both 77 and 277 K. The sulfur ligand is conceived as the Cys-43 sulfur, and the low-$Z$ ligands are conceived as one nitrogen (His-68) and three oxygens (water and Glu-154). Two alternative explanations for the additional low-$Z$ ligand found compared with the prediction of the model could be considered. One is that the second water molecule possibly present in the zinc environment (Eklund et al., 1985) is coordinated to zinc [cf. a similar suggestion for carbonic anhydrase (Clementi et al., 1979)]; the other is that Glu-154 is coordinated with two rather than one of its carboxylate oxygens [cf. carboxypeptidase (Rees et al., 1981)]. Neither of these explanations affects the main conclusion of the present study, which is that there is only one cysteine sulfur ligand to zinc in sorbitol dehydrogenase, sustaining the ligand arrangement proposed in the model (Eklund et al., 1985) as a strong possibility. This study is the first experimental check on this model, and the evidence presented for its correctness is also evidence for the validity of predictive techniques used in constructing the model (computer graphics fitting of the amino acid sequence to the crystallographically derived structure of a different but homologous protein), techniques which are crucially important in molecular biology and protein engineering where predictions of the detailed tertiary structures of proteins are essential.

Regarding bound metals, the importance of identifying the ligands to functional metal atoms constrasts with the paucity of techniques that provide direct access to the necessary information. Commonly, a high-resolution crystallographic structure may not be available for the particular protein in question, and the possibility of applying EXAFS in such cases becomes attractive. The present study, concerning an active site zinc atom, illustrates the strengths and limitations of EXAFS in this respect. Thus, information relating directly to the intimate environment of the zinc atom is obtained, and interpretation can be attempted in terms of independently predicted structures. The use of EXAFS to distinguish between a limited number of defined alternative structures can be productive, as in the present case in which the possibility of more than one sulfur ligand to the zinc atom was essentially excluded. However, an overrestrictive selection of alternative structures for evaluation should clearly be avoided, because structures involving an unusual bond length or an extra ligand may be possible within a protein and, as illustrated in the present case when 5-coordinate zinc was entertained as a possibility, may fit the EXAFS findings better than more obvious model structures. A powerful further approach involves site-directed mutagenesis to change specific residues putatively involved in ligation and EXAFS studies also of the mutant proteins.

## ACKNOWLEDGMENTS

We thank Irene Wood for skilled technical assistance, Christa Jeffery for expert preparation of the manuscript, M. Tollenaar and J. L. den Boesterd for preparing the figures, and Prof. C.-I. Brändén, Dr. G. P. Diakun, Dr. H. Eklund, Prof. C. D. Garner, Dr. S. S. Hasnain, Prof. H. Jörnvall, and Dr. A. T. Steel for stimulating discussions.

## REFERENCES

Abrahams, I. L., Bremner, I., Diakun, G. P., Garner, C. D., Hasnain, S. S., Ross, I., & Vasak, M. (1986) *Biochem. J. 236*, 585–589.

Baines, J. T., Garner, C. D., Hasnain, S. S., & Morrell, C. (1986) *Nucl. Instrum. Methods A246*, 565–568.

Brändén, C.-I., Jörnvall, H., Eklund, H., & Furugren, B. (1975) *Enzymes (3rd Ed.) 11*, 103–190.

Citrin, P. H., Eisenberger, P., & Kincaid, B. M. (1976) *Phys. Rev. Lett. 36*, 1346–1349.

Clementi, E., Corungiu, G., Jonsson, B., & Romano, S. (1979) *FEBS Lett. 100*, 313–317.

Cremers, T. L., Bloomquist, D. R., Willett, R. D., & Crosby, G. A. (1980) *Acta Crystallogr. B36*, 3097–3099.

Diakun, G. P., Fairall, L., & Klug, A. (1986) *Nature 324*, 698–699.

Eisenberger, P., & Lengeler, B. (1980) *Phys. Rev. B 22*, 3551–3561.

Eklund, H., Horjales, E., Jörnvall, H., Brändén, C.-I., & Jeffery, J. (1985) *Biochemistry 24*, 8005–8012.

Feiters, M. C., Little, C., & Waley, S. G. (1986a) *J. Phys. 12-47-C8*, 1169–1172.

Feiters, M. C., Hasnain, S. S., Groeneveld, C. M., Canters, G. W., van Rijn, J., Reedijk, J., Dahlin, S., & Reinhammar, B. (1986b) *J. Phys. 12-47-C8*, 1173–1176.

Feiters, M. C., Navaratnam, S., Al-Hakim, M., Allen, J. C., Spek, A. L., Veldink, G. A., & Vliegenthart, J. F. G. (1988) *J. Am. Chem. Soc. 110*, 7746–7750.

Garner, C. D., & Feiters, M. C. (1987) in *Biophysics and Synchrotron Radiation* (Bianconi, A., & Congiu-Castellano, A., Eds.) pp 136–146, Springer-Verlag, Berlin.

Greaves, G. N., Diakun, G. P., Quinn, P. D., Hart, M., & Siddons, D. P. (1983) *Nucl. Instrum. Methods 208*, 335–339.

Groeneveld, C. M., Feiters, M. C., Hasnain, S. S., van Rijn, J., Reedijk, J., & Canters, G. W. (1986) *Biochim. Biophys. Acta 873*, 214–227.

Gurman, S. J., Binsted, N., & Ross, I. (1984) *J. Phys. C. 17*, 143–151.

Gurman, S. J., Binsted, N., & Ross, I. (1986) *J. Phys. C. 19*, 1845-1861.
Hasnain, S. S., Quinn, P. D., Diakun, G. P., Wardell, E. M., & Garner, C. D. (1984) *J. Phys. E 17*, 40-43.
Hasnain, S. S., Wardell, E. M., Garner, C. D., Schlösser, M., & Beyersmann, D. (1985) *Biochem. J. 230*, 625-633.
Jeffery, J., & Jörnvall, H. (1988) *Adv. Enzymol. 61*, 47-106.
Jeffery, J., Cummins, L., Carlquist, M., & Jörnvall, H. (1981) *Eur. J. Biochem. 120*, 229-234.
Jeffery, J., Cederlund, E., & Jörnvall, H. (1984a) *Eur. J. Biochem. 140*, 7-16.
Jeffery, J., Chesters, J., Mills, C., Sadler, P. J., & Jeffery, J. (1984b) *EMBO J. 3*, 357-360.
Jörnvall, H., von Bahr-Lindström, H., & Jeffery, J. (1984) *Eur. J. Biochem. 140*, 17-23.
Jörnvall, H., Persson, B., & Jeffery, J. (1987) *Eur. J. Biochem. 167*, 195-201.
Pettifer, R. F., Foulis, D. L., & Hermes, C. (1986) *J. Phys. 12-47-C8*, 545-550.
Phillips, J. C., Bordas, J., Foote, A. M., Koch, M. H. J., & Moody, M. F. (1982) *Biochemistry 21*, 830-834.
Rees, D. C., Lewis, M., Honzatko, R. B., Lipscomb, W. N., & Hardman, K. D. (1981) *Proc. Natl. Acad. Sci. U.S.A. 78*, 3408-3412.
Sayers, D. E., Stern, E. A., & Lytle, F. W. (1971) *Phys. Rev. Lett. 27*, 1204-1207.
Stern, E. A. (1974) *Phys. Rev. B 10*, 3027-3037.
Strange, R. W., Blackburn, N. J., Knowles, P. F., & Hasnain, S. S. (1987) *J. Am. Chem. Soc. 109*, 7157-7162.
Yachandra, V., Powers, L., & Spiro, T. G. (1983) *J. Am. Chem. Soc. 105*, 6596-6604.
Zeppezauer, M., Haas, C., Maret, W., Hermes, C., & Pettifer, R. F. (1986) *J. Phys. 12-47-C8*, 1165-1168.

# Distamycin Paradoxically Stimulates the Copying of Oligo(dA)·Poly(dT) by DNA Polymerases†

Aliza Levy, Pnina Weisman-Shomer, and Michael Fry*
*Rappaport Institute for Research in the Medical Sciences and Unit of Biochemistry, Faculty of Medicine, Technion—Israel Institute of Technology, P.O. Box 9649, Haifa 31096, Israel*
*Received February 14, 1989; Revised Manuscript Received May 11, 1989*

ABSTRACT: Distamycin A, a polypeptide antibiotic, binds to dA·dT-rich regions in the minor groove of B-DNA. By virtue of its nonintercalating binding, distamycin acts as a potent inhibitor of the synthesis of DNA both in vivo and in vitro. Here we report that distamycin paradoxically stimulates *Escherichia coli* DNA polymerase I (pol I), its large (Klenow) fragment, and bacteriophage T4 DNA polymerase to copy oligo(dA)·poly(dT) in vitro. It is found that distamycin increases the maximum velocity ($V_{max}$) of the extension of the oligo(dA) primer by pol I without affecting the Michaelis constant ($K_m$) of the primer. Gel electrophoresis of the extended primer indicates that the antibiotic specifically increases the rate of addition of the first three dAMP residues. Lastly, in the presence of both distamycin and the oligo(dT)-binding protein factor D, which increases the processivity of pol I, a synergistic stimulation of polymerization is attained. Taken together, these results suggest that distamycin stimulates synthesis by increasing the rate of initiation of oligo(dA) extension. The stimulatory effect of distamycin is inversely related to the stability of the primer–template complex. Thus, maximum stimulation is exerted at elevated temperatures and with shorter oligo(dA) primers. That distamycin increases the thermal stability of [$^{32}$P](dA)$_9$·poly(dT) is directly demonstrated by electrophoretic separation of the hybrid from dissociated [$^{32}$P](dA)$_9$ primer. It is proposed that by binding to the short primer–template duplex, distamycin stabilizes the oligo(dA)·poly(dT) complex and, therefore, increases the rate of productive initiations of synthesis at the primer terminus.

Distamycin A, a nonintercalating oligopeptide antibiotic, binds to clusters of dA·dT base pairs within the minor groove of double-stranded B-form DNA [for reviews, see Zimmer (1975) and Zimmer and Wahnert (1986)]. Footprinting analyses with methidiumpropyl-EDTA·Fe(II) (Van Dyke et al., 1982; Van Dyke & Dervan, 1982) and with nuclease (Portugal & Waring, 1987) indicate that a minimum size of four dA·dT base pairs is required for the binding of distamycin to DNA. Upon binding of distamycin or its close relative netropsin to DNA, the inherently curved antibiotic molecules force open the minor groove and bend back the helix axis by 8° (Kopka et al., 1985; Ekambareswara et al., 1988). Further, an increased nuclease susceptibility of regions in the vicinity of the antibiotic binding site suggests that in addition to its direct effect on the structure of the bound base cluster, distamycin introduces structural variations in flanking base stretches (Fox & Waring, 1984).

Distamycin and netropsin are potent inhibitors of the growth of bacteria and viruses as well as of plant and animal cells, both exhibit antimitotic and antitumor activity, and both are cytotoxic [reviewed by Zimmer and Wahnert (1986)]. These effects of the antibiotics are mostly due to the inhibition of RNA and DNA synthesis consequent to their binding to the DNA template. In addition to blocking the in vitro activity of various RNA polymerases (Zimmer et al., 1971; Puschendorf et al., 1974; Muller et al., 1974; Jaros-Kaminska, 1981), distamycin was shown to inhibit the in vitro activity

† This study was supported by the Fund for Basic Research administered by the Israel Academy of Sciences and Humanities and by a grant from the Loewengart Research Fund administered by the Technion Vice President for Research.

0006-2960/89/0428-7262$01.50/0 